ORIGINAL RESEARCH

# Green Approach to Beckmann Rearrangement of Cyclohexanone Oxime Using Nanostructured ZSM-5 Zeolite

**Article History**
Received: 10-Jun-2025
Revised: 20-Jul-2025
Accepted: 30-Jul-2025
Published: 20-Sep-2025

**L. Selva Roselin[a,*], R. Savidha[b], Walaa Alharbi[a], Khadijah H. Alharbi[a], Ruey Chang Hsiao[c], Sankar Ganesh Ramaraj[d], Rosilda Selvin[e]**

**Abstract:** The catalytic liquid-phase Beckmann rearrangement of cyclohexanone oxime to ε-caprolactam has been effectively achieved using ZSM-5 nanoparticles as catalysts. Comprehensive characterization of the catalysts was performed by utilizing techniques such as DLS, XRD, FT-IR, $N_2$ adsorption–desorption isotherms and NMR analysis. A systematic investigation of key reaction parameters, including the concentration of cyclohexanone oxime, catalyst loading, reaction temperature, and catalyst reusability, was conducted to optimize the catalytic process. The results demonstrate that the ZSM-5 nanoparticles aged at 80°C for 24 h and calcined at 550°C for 5 h (denoted as ZSM-5(50)-24/c) exhibited superior catalytic performance, achieving the highest conversion of cyclohexanone oxime and exceptional selectivity for ε-caprolactam under optimized conditions. The optimum reaction conditions are 0.10 g of ZSM-5(50)-24/c catalyst, cyclohexanone oxime concentration of 100 mmol and the reaction temperature of 120°C. This catalytic system offers notable advantages, including environmental sustainability, straightforward separation, and efficient catalyst recovery and recyclability. These features make it a promising approach for industrial applications in ε-caprolactam production, aligning with the green chemistry principle.

**Keywords:** Amorphous ZSM-5 nanoparticles; Beckmann rearrangement; Cyclohexanone oxime; ε-caprolactam; Zeolite.

a Department of Chemistry, Science and Arts College, King Abdulaziz University, Rabigh 21911, Saudi Arabia

b Department of Chemistry, Providence College for Women (Autonomous), Spring Field, Bandishola, Coonoor, Tamil Nadu 643104, India

c Department of Semiconductor Engineering, Lunghwa University of Science and Technology, No. 300, Section 1, Wanshou Rd, Guishan District, Taoyuan City, Taiwan 333

d Department of Bioengineering, Graduate School of Engineering, The University of Tokyo, 7-3-1 Hongo, Tokyo 113-8656, Japan

e Nanomaterials Application Laboratory, The Institute of Science, Dr. Homi Bhabha State University, Mumbai 400032, India

* **Corresponding Author's Email:** slous@kau.edu.sa



## 1. INTRODUCTION

The Beckmann rearrangement is a chemical reaction that involves the rearrangement of cyclohexanone oxime into caprolactam, which is the intermediate in the production of fibers and resins (Kirk-Othmer, 1992; Kiely-Collins et al., 2018; Jang et al., 2019). In addition, this rearrangement is the most relevant large-scale industrial process, contributing to the synthesis of a diverse range of functional molecules. The literature unequivocally shows that nylons are the second most produced synthetic fiber in terms of volume, and caprolactam is ranked 50th out of the top 50 compounds (Corma et al., 1991). Conventionally Beckmann rearrangement was carried out using catalytic amount of concentrated sulphuric acid. Despite having a high caprolactam selectivity, sulfuric acid has a number of drawbacks when used in different industrial processes, such as the significant by-product creation of low-value inorganic salts, transposition issues, heat evolution during neutralization, corrosion of equipment and the process causes serious environmental pollution (Hölderich et al., 1997; Kent J.E. Riegel, 1983). The aforementioned challenges are addressed by numerous research teams and a variety of solid acid catalysts are explored as alternatives to concentrated sulfuric acid. To

begin with metal oxides such as $ZrO_2$ (Xu et al., 1999), $Al_2O_3$ (Curtin, 1992), $V_2O_5/SnO_2$ (Wang et al., 2013) and $TiO_2$–$ZrO_2$ (Mao, 2001) are studied. Despite the high activity exhibited by the above-mentioned catalysts is limited by the catalyst deactivation and poor selectivity after a few hours. Several solid acid catalysts, including boron oxide on various carriers (Curtin et al., 1993; Sato et al., 1986), tantalum oxide (Ushikubo and Wada, 1994), silica-titania (Katada et al., 1995), silica-supported niobium (Maronna et al., 2016) and niobium oxide supported on titania (Anilkumar and Hoelderich, 2012) have been studied for the vapor-phase Beckmann rearrangement. The need for high temperatures and the catalyst's deactivation as a result of coke production are two significant limitations of the vapor-phase process (Ishida et al., 2003). The remarkable qualities of ionic liquids (ILs), such as their large solvent capacity, broad liquid temperature range, and minimal vapor pressure, have attracted a lot of attention (Poole, 2004). Their non-hazardous nature renders organic synthesis more environmentally friendly (Welton and Wasserscheid, 2008; Davis Jr and Fox, 2003). In recent years, they have found considerable success in the Beckmann rearrangement (Dupont et al., 2002; Wasserscheid and Keim, 2000). However, traditional catalysts like $P_2O_5$, $PCl_5$, other Lewis acids, and Metaboric acid, coupled with high temperatures (75–120°C), have remained indispensable (Ren et al., 2001; Chandrasekhar and Gopalaiah, 2003). However, these rearrangements encounter certain challenges, including the challenge of separating products from ionic liquids was difficult to achieve and the environmental pollution resulting from the utilization of phosphorated compounds.

Liquid-phase Beckmann rearrangement process takes place at moderate conditions and could afford good results. Hence it was studied over various catalysts such as sulfamic acid (Wang, et al., 2004), anhydrous oxalic acid (Chandrasekhar and Gopalaiah, 2003), solid metaboric acid (Chandrasekhar and Gopalaiah, 2002), tetrabutylammonium perrhenate (Narasaka et al., 1993), boron trifluoride etherate, and chlorosulfonic acid–dimethyl formamide reagent (Davis Jr and Fox, 2003).

Clean and ecologically friendly technologies require the development of selective heterogeneous catalysts using zeolites and molecular sieves (Corma, 2003). The architecture of microporous zeolites allows molecules to diffuse through a variety of interconnected channels and cages under controlled conditions, and can be made in a range of crystalline structures (Smith, 1988), different level of ion exchange (Jacobs, 1977) and ranges of framework Si/Al ratios (Beaumont and Barthomeuf, 1972). It is also feasible to design the synthetic procedure to direct the creation of active sites that exhibit a particular catalytic function by enabling Bronsted and Lewis acid sites engineered within the framework (Choi et al., 2006; Potter et al., 2014; Dusselier et al., 2015; Leithall et al., 2013).

Numerous research endeavors have been pursued to augment the inherent characteristics of zeolites, thereby enhancing their efficacy and versatility as robust acid catalysts across diverse industrial processes (Raja et al., 2014; Dai et al., 1996; Sahu and Sakthivel, 2021; Wang et al., 2023; Shabana et al., 2024; Nimisha et al., 2024). Different zeolites, including Faujasites (Aucejo et al., 1986), ZSM-5 (Yashima et al., 1997), and Beta (Dai et al., 1996) Silicalite-1 (Hölderich et al., 1997), HY (Dai et al., 1999), TS-1 (Palkovits et al., 2009), and B-MFI (Röseler et al., 1996), were investigated for the Beckmann Rearrangement and have been published. Liquid phase Beckman rearrangement of cyclohexanone oxime over Zeolite Y and ZSM-5 and the study reveals that the acidic characteristics of the zeolites at moderate temperatures yield high conversions and moderate-to-good selectivity of the desired product (Corma et al., 1991). Aligning different hydroxyl groups and silanol nests on the zeolite catalysts' surface improves the production of ε-caprolactam, according to a rearrangement carried out over modified beta zeolite (Thangaraj et al., 1992). Zang et al., observed a notable trend in their investigation of the reaction over phosphorus-modified Si-MCM-41 catalyst: as the P content increased, weak acid sites became more prevalent, consequently boosting catalytic activity. The primary active sites for the Beckmann rearrangement were identified as the P–OH groups (Zhang et al., 2010). Moreover, their study unveiled a potentially superior approach for enhancing selectivity: grafting acid hydroxyl groups to mask Si–OH groups. Liquid phase Beckmann Rearrangement using a combination of sophisticated in situ spectroscopic characterization techniques, including quasi-elastic and inelastic neutron scattering, over SAPO-37 was investigated in order to comprehend the role of diffusion in catalysis and to design highly active, selective, and stable industrial heterogeneous catalysts (Potter et al., 2017). The findings clarify how molecular diffusion and active sites interact in single-site

heterogeneous catalysts, which is important information for developing low-temperature, environmentally friendly catalytic processes. Quantum-chemical studies carried out by Sirijaraensre et al. further confirm the crucial function provided by silanol groups (Sirijaraensre and Limtrakul, 2009). Several recent in situ spectroscopic investigations focused on the mechanism of the Beckmann rearrangement of oximes, wherein surface hydroxyl groups with different chemical properties and local structures, such as isolated SiOH groups and SiOH nests, were analyzed (Marthala et al., 2010; Lezcano-González et al., 2009; Marthala et al., 2008). The majority of research generally agreed that because bridging hydroxyl groups promote unwanted secondary reactions and catalyst deactivation, they are less selective but more active than weakly acid silanol groups (Ichihashi et al., 2003; Thangaraj et al., 1992). Despite the various benefits, an acceleration of catalyst deactivation is seen due to the slow mass transfer from and to the active sites located within the micro-pores during Beckmann rearrangement (Ando et al., 1986; Flowers et al., 1984). The reduction in the particle size of zeolites in the nanoscale level increases the surface area of the zeolite crystals and reduces the diffusion path length (Thorat et al., 1992; Selvin et al., 1999, 2001). Hierarchical Beta zeolite featuring intra-crystalline mesoporosity demonstrated an extended lifetime compared to conventional Beta zeolite. Its enhanced catalytic performance is credited to the hierarchical pore architecture and well-balanced acidity (Zhang et al., 2018).

Nano-zeolites have been identified as promising candidates for numerous organic reactions, as documented in the literature (Selvin et al., 2008; Polshettiwar and Varma, 2010). According to published research, hierarchical porous zeolites—which possess micro, meso, and macro pores can serve as a more effective substitute for materials with mass transfer restrictions (Elings et al., 1998; Centi and Perathoner, 2011; Yadav and Joshi, 2001). Khayyat et al. (2017) studied the Beckmann rearrangement of cyclohexanone oxime on hierarchical nanocrystalline TS-1 catalyst and the results reveals superior activity, selectivity towards the desired products at mild reaction conditions and excellent reusability. Deng et al. (2012) studied the relationship between structure and catalytic efficiency of nanosized silicalite-1 zeolites for the vapor-phase Beckmann rearrangement of cyclohexanone oxime. The reports exhibit higher catalytic activity as well as better caprolactam selectivity and catalyst stability of nanosized silicalite-1. Structure performance relationship of silicalite1 nanosheets in vapor phase. Beckmann rearrangement of cyclohexanone oxime was studied by Ge et al. (2021). Though the catalytic activity of Bulky silicalite-1 for vapor phase Beckmann rearrangement of cyclohexanone oxime is higher, it is accompanied by rapid catalyst deactivation. Recent literature on zeolite catalytic systems for the Beckmann rearrangement has shown significant improvements in catalytic activity; however, further validation is still needed regarding their activity and selectivity (Chang et al., 2020; Park et al., 2023; Yin et al., 2024; González-Camuñas et al., 2024). Hence, the preparation of Silicate-1 catalyst with tunable morphology which changed from 3-dimentional bulk to 2-dimentional nanosheets was done. The number of active sites silanol nests is linearly correlated to the external surface area, thereby increasing the catalytic activity and the long-life time with high coke tolerance capacity was reported (Li et al., 2005).

It is widely acknowledged that zeolites' morphological and chemical properties are crucial in influencing both their catalytic activity and product selectivity. In the present study, X-Ray-amorphous ZSM-5 Nanoparticles for Beckmann rearrangement of cyclohexanone oximeis studied.

## 2. MATERIALS AND METHODS

### 2.1. Chemicals

Tetraethoxysilane (TEOS), aluminum isopropoxide (AlP), and tetrapropylammonium hydroxide (TPAOH, 40% aq) were procured from Merck and utilized without additional purification. Cyclohexanone oxime and benzonitrile were acquired from Aldrich, USA.

### 2.2. Synthesis of Nanoparticles of ZSM-5 (Si/Al = 50)

Nanocrystalline ZSM-5 (Si/Al = 50) was prepared from a hydrolyzed clear sol of TPAOH-AlP-TEOS-$H_2O$, at room temperature. Typically, 0.61 g of AIPO was transferred to a 250 ml PP (polypropylene) bottle containing 19.02 g of TPAOH (40% aq.). The

solution was stirred on a magnetic stirrer for approximately 40 minutes until achieving clear solution. Then, 31.24 g of TEOS (tetraethoxysilane, Merck) and 316.2 g of DI water were added to the clear solution. TEOS underwent hydrolysis through vigorous stirring at 25°C for about 2 h, resulting in a clear solution. The molar composition of the resulting sol was 0.2 TPAOH/1 TEOS/0.02 AlPO/40 $H_2O$ with a pH of 11.02.

The clear sol was concentrated to 26.92 g (transparent viscous sol, mole ratio of water after concentration was 4.06) using a rotary evaporator at 80°C for 105 min. pH of 12.12 was noted for the final concentrated NPs solution. The transparent, viscous solution was divided into three portions, each weighing 8.06 g, and labeled as I, II, and III. Samples II and III were heated at 80°C for 24 and 48 h, respectively, while sample I remained unheated. A clear solution was obtained for samples I and II. The samples underwent calcination at 550°C for 5 h (heating rate of 2°C/min). The uncalcined samples that were unaged and aged for 24 h and 48 h were denoted as ZSM5(50)-0, ZSM5(50)-24, and ZSM5(50)-48, respectively. These samples after calcination were labeled as ZSM5(50)-0/c, ZSM5(50)-24/c, and ZSM5(50)-48/c.

### 2.3. Characterization

Dynamic Light Scattering (DLS) study was done using a Malvern Zetasizer Nano ZS instrument. Powder X-ray diffraction patterns were recorded using a Rigaku 2000 diffractometer equipped with Cu-Kα radiation (wavelength λ = 1.5418 Å). The FTIR spectrum of the catalyst was recorded using the KBr wafer technique (1.2% w/w) on a Perkin Elmer FTIR instrument. Nitrogen sorption studies were done using a Micromeritics ASAP 2020 instrument at 77.8 K. Before recording the measurements, the catalysts were vacuum-degassed. $^{27}Al$ magic angle spinning (MAS) NMR spectra were recorded on a Bruker DSX-300 spectrometer, equipped with 4- and 7-mm MAS probes, with $^{27}Al$ resonance frequencies of 78.17 MHz. All $^{27}Al$ MAS NMR spectra were obtained with small flip angles of approximately 15 degrees and with a recycle delay of 1 s. In order to favor a symmetric environment around the aluminum nucleus, all samples were hydrated under atmospheric conditions before acquiring the NMR spectra. A π/6 excitation pulse. $^{27}Al$ and $^{29}Si$ chemical shifts were externally referenced to $Al(H_2O)_6^{3+}{}_{(aq)}$ at 0.0 ppm.

### 2.4. Catalytic Studies

The liquid-phase Beckmann rearrangement of cyclohexanone oxime was conducted at atmospheric pressure within a 100 ml glass reactor. The reaction mixture comprised cyclohexanone oxime dissolved in benzonitrile solvent, alongside ZSM-5 nanoparticles serving as the catalyst. In a standard experiment, the reaction mixture comprised cyclohexanone oxime (100 mmol) dissolved in 20 ml of benzonitrile solvent. A freshly activated catalyst (0.10 g) was introduced into the flask containing the mixture, which was then heated at a constant temperature of 120°C in an oil bath for 5 h. Throughout the reaction, the mixture was stirred magnetically under a stream of nitrogen. The reaction mixture was periodically withdrawn and subjected to centrifugation. Subsequently, it was analyzed using a China Chromatography 8900 equipped with a capillary column (cross-linked 5% phenylmethyl silicone) and a flame ionization detector (FID). Identification of reaction products was confirmed through GC-MS analysis. Conversion is expressed as the percentage of cyclohexanone converted into the product.

## 3. RESULTS AND DISCUSSION

### 3.1. Dynamic Light Scattering (DLS) Analysis

The particle size distribution in concentrated precursor sol aged at 80°C for 0, 24, and 48 h for ZSM5(50)-0, ZSM5(50)-24, and ZSM5(50)-48 is depicted in **Fig. 1**. The image illustrates a monomodal distribution. The average size obtained from the DLS data exhibits a gradual rise over the aging period, with the rate of increase stabilizing notably after 24 h. A new population, approximately 29 nm in size, began emerging after 24 h of ageing. Over the next 18 h, this population grew to around 30 nanometers, coexisting with a persistent population of sub-colloidal particles around 5 nm in size. By the time the sol had aged for 48 h, a final population centered at approximately 35 nm had formed. The presence of primary particles ranging from 3 to 5 nm in a clear zeolite precursor sol has been acknowledged (Regev et al., 1994; De Moor et al., 1999). Increasing the initial silica concentration in the concentrated precursor sol promotes the limited growth of aggregates during the aging process, unlike the nano-zeolites produced using lower silica concentrations. This suggests that

more aggregates were likely nucleated initially. Consequently, their growth might have consumed all primary units within the first 24 h, leaving insufficient nutrients for further growth.

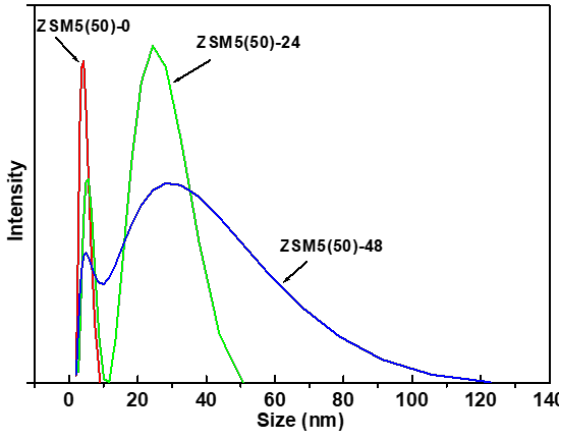


**Figure 1.** DLS curves for colloidal suspensions containing ZSM-5 zeolites after aging at different times.

## 3.2. XRD Analysis

The XRD patterns of the ZSM-5 nanoparticles ZSM-5(50)-0/c, ZSM-5(50)-24/c, and ZSM-5(50)-48/c are presented in **Fig. 2**. The diffraction pattern of the catalysts is notably similar to that of amorphous silica, except a distinct broad peak at 2θ ranging between 3 and 6 degrees. The catalysts ZSM-5(50)-0/c, ZSM-5(50)-24/c, and ZSM-5(50)-48/c exhibit peak maxima at 2θ = 3.5°, 3.5°, and 5°, respectively. Previous studies have reported observing this low-angle peak in their investigations of nanosized silicalite (Ravishankar et al., 1999; Kragten et al., 2003). According to Kremer et al., (2002), this peak serves as evidence of the intercalation of CTAB, resulting in the formation of a layered structure and subsequent scattering by small particles. Some study groups suggest that rather than being connected to the interior atomic structure of the particle, this is probably a feature associated with small particle sizes (Kragten et al., 2003). In the present study, a low-angle peak is observed even without the presence of added surfactant. This suggests that it might be solely attributed to scattering by the small particles rather than being associated with the layered structure. Jacobs, in his studies on X-ray evidence of amorphous zeolites, applied the Scherrer formula (Jacobs et al., 1981). He determined that to detect an X-ray diffraction peak at 2θ = 10°, the crystallite sizes should be approximately 8 nm. This implies that the materials must possess crystals with fewer than 4-unit cells and include ZSM-5 crystals smaller than 8 nm within an amorphous matrix.

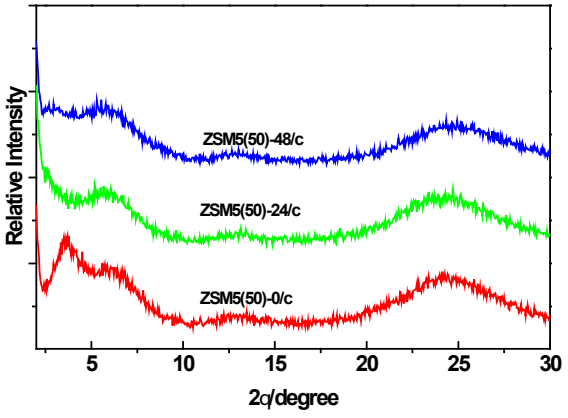


**Figure 2.** XRD patterns of nanoparticles of calcined samples of ZSM-5 after aging at different times.

## 3.3. FTIR Analysis

The ZSM-5 catalyst used in the present study appears X-ray amorphous, indicating the presence of very small zeolite nuclei with sizes below the detection limit of X-ray diffraction. Similar findings have been reported in the literature (Jacobs et al., 1981), where zeolite materials with such tiny nuclei often exhibit X-ray amorphous characteristics. To further investigate the crystallinity, FT-IR spectroscopy was employed, revealing a significant degree of structural order. Literature also suggests that crystals with fewer than four-unit cells contain only a few repeating units of the zeolite framework, indicative of nanocrystalline or poorly crystalline materials. The strong skeletal vibration bands observed in the FT-IR spectra support the existence of zeolitic structural units, even in agglomerates composed of just a few unit cells. **Fig. 3** illustrates the FTIR spectra of ZSM-5 nanoparticles: ZSM-5(50)-0/c, ZSM-5(50)-24/c, and ZSM-5(50)-48/c. The band observed at 950 $cm^{-1}$ corresponds to the localized Si–OH stretching mode. Spectral regions ranging from 750 to 850 $cm^{-1}$ and 500 to 650 $cm^{-1}$ are indicative of the ring structure of silica, while a broad band around 550 $cm^{-1}$ suggests the presence of small ring structures, with relatively lower intensity. The band at approximately 540 $cm^{-1}$ is attributed to the double 5–rings of crystalline ZSM-5. In fully crystalline ZSM-5, the 550 $cm^{-1}$ band comprises approximately 70% of the Si–O bending region at 450 $cm^{-1}$.

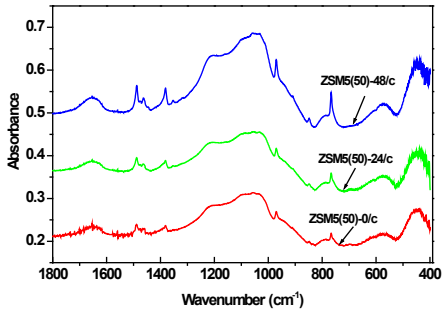


**Figure 3.** FTIR spectrum of nanoparticles of calcined samples of ZSM-5 after aging at different times.

### 3.4. ASAP Analysis

Nitrogen adsorption-desorption studies were conducted at 77.4 K to probe the porous structure of ZSM-5 nanoparticles. **Fig. 4** illustrates the nitrogen physisorption isotherms of ZSM-5 (50)-NP.0/c, ZSM-5 (50)-NP.24/c, and ZSM-5 (50)-NP.48/c. The findings indicate that the samples exhibit microporosity. Specifically, the micropore volume of ZSM-5 (50)-NP.0/c is typically one-third of that observed in microporous ZSM-5, whereas ZSM-5(50)-24/c and ZSM-5 (50)-48/c show micropore volumes typically two-thirds that of microporous ZSM-5. This suggests a partial crystalline nature of the samples. There is no discernible difference in adsorption between the ZSM-5(50)-24/c and ZSM-5(50)-48/c samples. A noteworthy observation is the lower micropore volume in nanoparticles of ZSM-5 compared to their micrometer-sized counterparts. This phenomenon aligns with the smaller crystal size of the nanoparticles, resulting in a higher external surface area at the expense of microporosity. The BET surface areas are found to be 665, 646 $m^2/g$ and 632 $m^2/g$ for samples ZSM-5(50)-0/c, ZSM-5(50)-24/c and ZSM-5(50)-48/c, respectively.

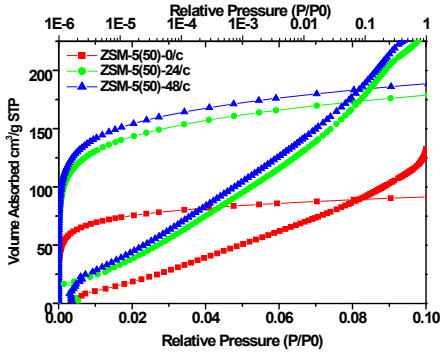


**Figure 4.** $N_2$ adsorption–desorption isotherms of ZSM-5 nanoparticles after aging at different times.

### 3.5. NMR Analysis

Nucleation and crystal growth processes are expected to be significantly impacted by the presence of aluminum species in the zeolite synthesis mixture. Investigating the coordination of these aluminum species can provide valuable insights into the underlying mechanisms driving crystallization. **Fig. 5** illustrates the $^{27}Al$ MAS-NMR spectrum of the ZSM-5(50)-0 and ZSM-5 (50)-24. Aluminum that is tetrahedrally coordinated in the framework is responsible for a signal at about 51 ppm. A material known as zeogrid is synthesized by precipitating a suspension of nano slabs with cetyltrimethylammonium bromide (Aerts et al., 2004). The as-synthesized sample exhibits predominantly tetrahedrally coordinated aluminum, while the calcined sample reveals additional framework aluminum. Van Grieken et al. demonstrated in their study on the crystallization progress of ZSM-5 nanoparticles, the tetrahedral aluminum was present in their amorphous materials before the onset of crystallization (Van Grieken, 2000). Furthermore, upon calcination, the partially crystalline samples exhibited a fraction of octahedral aluminum. In the present study, both the unaged ZSM-5(50)-0 and aged ZSM-5(50)-24 exhibit aluminum in their frameworks even before assembly.

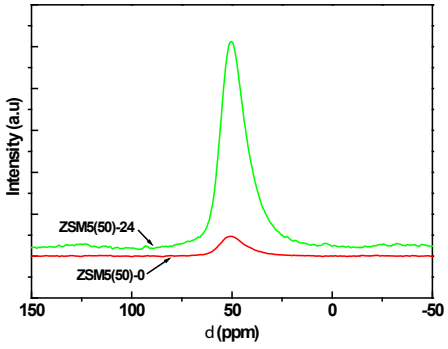


**Figure 5.** $^{27}Al$ MAS NMR spectra of ZSM-5 NPs.

### 3.6. Catalytic Activity

The catalytic performance of ZSM-5 nanoparticles was systematically studied, employing ZSM-5(50)-0/c, ZSM-5(50)-24/c and ZSM-5(50)-48/c). In the liquid-phase Beckmann rearrangement of cyclohexanone oxime over ZSM-5 nanoparticle catalysts, ε-caprolactam is the predominant product, accounting for over 95% of the yield, while only a minor fraction, less than 5%, consists of cyclohexanone. Nonetheless, secondary compounds are typically found, primarily the equivalent ketones

 https://doi.org/10.37819/nanofab.10.2079

(cyclohexanone) that are produced when the oxime is hydrolysed (**Scheme 1**). No significant quantities of other products resulting from dehydrogenation or fragmentation were observed under our experimental conditions. However, secondary products, primarily corresponding ketones (such as cyclohexanone), formed via oxime hydrolysis, are typically detected. The reaction parameters, including ageing time, reaction temperature, catalyst quantity, and concentration of cyclohexanone oxime, were optimized and regeneration and reusability tests were conducted.

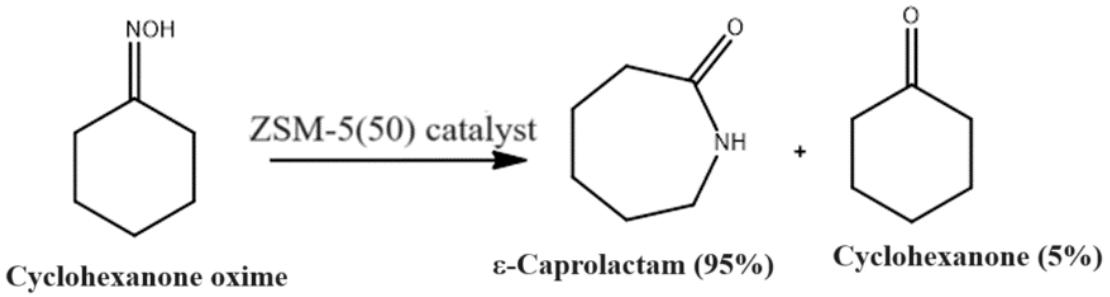


**Scheme 1.** Beckmann rearrangement of cyclohexanone oxime using the nanoparticles of ZSM-5 catalysts.

### *3.6.1. Comparison of Catalysts*

The catalytic efficiency of ZSM-5 nanoparticles (ZSM-5(50)-0/c, ZSM-5(50)-24/c, and ZSM-5(50)-48/c) synthesized using concentrated nano precursors with different aging times (0, 24, and 48 h at 80°C) was evaluated for the Beckmann rearrangement of cyclohexanone oxime under uniform reaction conditions. The performance of ZSM-5 nanoparticles, aged at 80°C for 24 h [ZSM-5(50)-24/c], exhibits a pronounced tendency towards the selective formation of caprolactam in the Beckmann rearrangement of cyclohexanone oxime. In the initial 5 h, there's a significant increase in the conversion of cyclohexanone oxime, jumping from 42.5% to 87.9% (**Fig. 6A**). This level remains steady thereafter; thus, subsequent experiments were conducted for 5 h each. The caprolactam selectivity peaked at two hours, and there was no discernible drop in selectivity over the course of the reaction time. Interestingly, extending the aging duration to 48 h doesn't significantly alter the percentage selectivity of caprolactam, which is clearly depicted in **Fig. 6B**. Conversely, the unaged concentrated nano precursor (ZSM-5(50)-0/c) displays lower activity in this context. Similarly, the conversion of cyclohexanone oxime is very less when compared to aged catalysts (**Fig. 6A**). During the aging process, the presence of a greater number of nucleation centers, shielded by $TPA^+$ ions, may contribute to enhanced accessibility for reactants and efficient removal of products. This phenomenon facilitates oxime conversion, thereby reducing the occurrence of side reactions and minimizing catalyst deactivation. This is consistent with previous studies that have shown significant activity and selectivity for Beckman rearrangement in mesoporous materials with an amorphous aluminosilicate or silicate framework and accessible channels larger than 20 Å (Conesa et al., 2007). The conversion of cyclohexanone oxime is significantly enhanced with the ZSM-5(50)-24 catalyst due to its substantial mesopore/external surface area (590 $m^2/g$). The conversion of cyclohexanone oxime is significantly enhanced with the ZSM-5(50)-24 catalyst due to its substantial mesopore/external surface area (590 $m^2/g$). This augmentation facilitates superior accessibility to the acid sites, reducing diffusion length and thereby promoting efficient adsorption/desorption of both reactants and products. As a result, more studies were conducted with ZSM-5(50)-24/c as the catalyst. The present study clearly demonstrates that the unique catalyst preparation method, which involves concentrating the nano precursors, results in the formation of X-ray amorphous materials with relatively high crystallinity, as confirmed by FT-IR analysis. These tiny crystals, due to their high surface area and improved accessibility, show a strong tendency for the selective formation of caprolactam, significantly outperforming conventional ZSM-5 and silicoalumina catalyst (Takahashi et al., 2004). Comparison of Nanostructured ZSM-5 Zeolite catalysts with silica-based catalysts in the Beckmann rearrangement of cyclohexanone oxime showed that with bare $SiO_2$ the reaction practically

does not proceed even at 323K (Marzianom et al., 2007). Catalysts such as $H_2SO_4/SiO_2$ (Marziano et al., 2007), silica-titania (Katada et al., 1995), silica-supported niobium (Maronna et al., 2016), and niobium oxide supported on titania (Anilkumar and Hölderich, 2012) exhibit lower activity and selectivity compared to nanostructured ZSM-5 zeolite catalysts. Furthermore, catalyst deactivation remains a significant challenge with these materials. Takahashi et al., (Takahashi et al., 2004) studied the Beckmann rearrangement using HZSM-5 zeolite and silica–alumina catalysts to evaluate their selectivity toward ε-caprolactam. The results indicate that acid sites located outside the well-ordered zeolite framework were responsible for catalyst deactivation. These sites, which may arise from defects or dealumination, can contribute to activity but often promote undesired side reactions and lead to faster deactivation due to coking or structural instability. The catalytic activity and selectivity of these conventional catalysts were significantly lower than those of the X-ray amorphous catalyst used in the present study for the Beckmann rearrangement of cyclohexanone oxime. The novelty of the current study lies in the superior regeneration capacity and sustained selectivity of the catalyst, suggesting the absence of significant extra-lattice acid sites in the material under investigation.

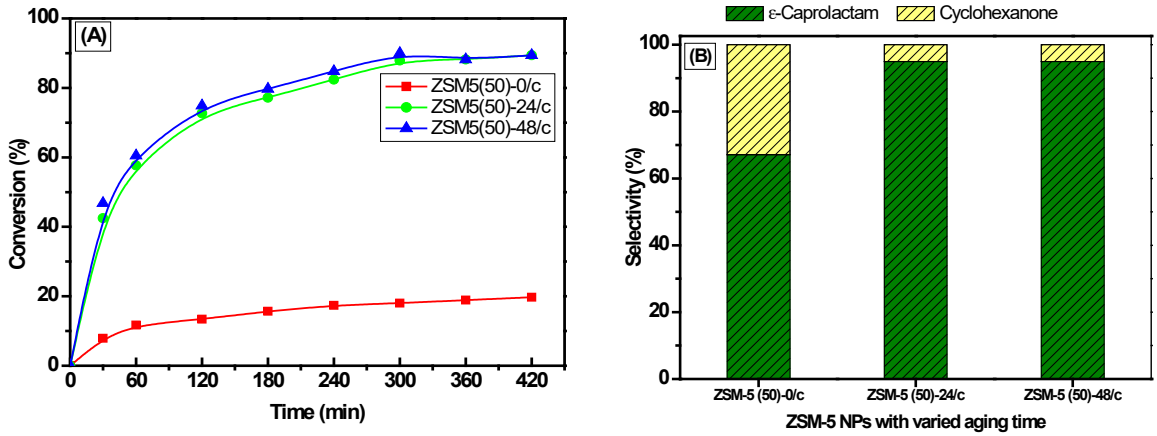


**Figure 6.** Effect of aging time on (A) % conversion and (B) % selectivity in Beckmann rearrangement of cyclohexanone oxime using ZSM-5 nanoparticles.
(Reaction conditions: catalyst-amount, 0.10 g; Concentration of cyclohexanone oxime (100 mmol); temperature-120°C; run time, 5 h; atmospheric pressure).

### *3.6.2. Effect of Concentration of Cyclohexanone Oxime*

In a catalytic reaction, maximizing the conversion of reactant molecules into products while minimizing the amount of catalyst used is crucial. Thus, optimizing the concentration of reactants for a given quantity of catalyst becomes imperative. The impact of reactant quantity on the rate of reaction was examined by adjusting the concentrations of cyclohexanone oxime within the range of 80 mmol to 120 mmol. The findings are illustrated as the percentage conversion of cyclohexanone oxime over time, with variations in initial concentrations of cyclohexanone oxime (**Fig. 7**). Starting from 21% for an initial concentration of 80 mmol, the conversion surged to 42.5% for 100 mmol, and further to 50.7% for 120 mmol after 30 minutes. Following 300 minutes of reaction time, the conversion continued to rise dramatically to 55.3%, 87.9%, and 90.1% for initial concentrations of 80 mmol, 100 mmol, and 120 mmol, respectively. This signifies a remarkable increase in the conversion of cyclohexanone oxime. Over the observed period, there's a noticeable decline in conversion percentage, attributable to an excess of molecules relative to the catalyst amount at higher initial concentrations of cyclohexanone oxime. Selectivity towards product formation remains negligible across the investigated range of cyclohexanone oxime concentrations. To facilitate further investigations, an optimal concentration of 100 mmol cyclohexanone oxime was established.

 https://doi.org/10.37819/nanofab.10.2079

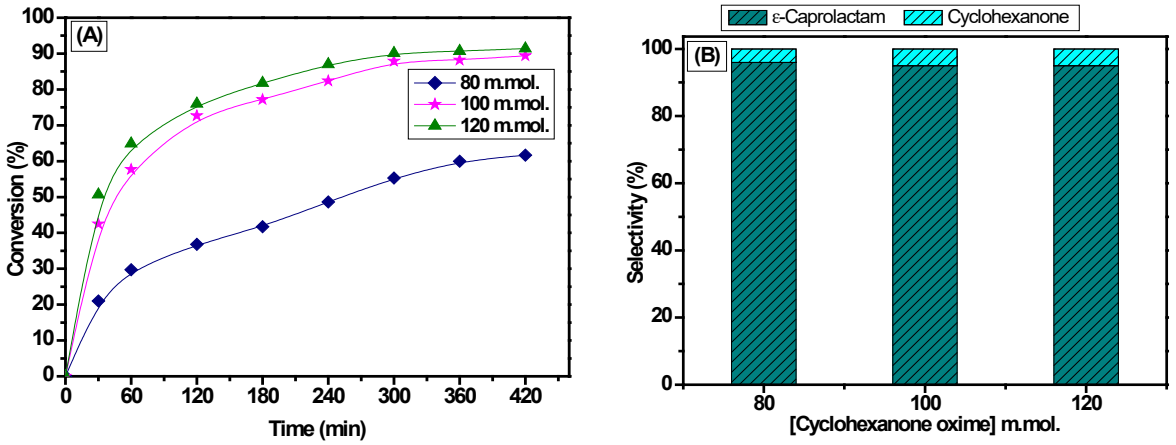


**Figure 7.** Effect of cyclohexanone oxime concentration on (A) % conversion and (B) % selectivity in Beckmann rearrangement of cyclohexanone oxime using ZSM-5 (50)-NP.24/c catalyst.
(Reaction conditions: catalyst, 0.10 g of ZSM-5 (50)-NP.24/c; temperature-120 oC; run time, 5 h; atmospheric pressure).

### 3.6.3. Effect of Ctalyst Quantity

**Fig. 8** shows the effect of catalyst quantity on the Beckmann rearrangement of cyclohexanone oxime at 120°C, using ZSM-5 (50)-NP.24/c catalyst throughout a range of 0.05–0.20 g. The conversion of cyclohexanone oxime demonstrated a direct correlation with the catalyst amount, attributed to the proportional augmentation in active sites. Notably, a substantial enhancement in the % conversion from 58.1% to 87.9 % was observed as the catalyst load increased from 0.05 to 0.10 g, respectively, at 300 minutes. However, the significance of this increase diminishes beyond 0.10 g, indicating that additional active sites fail to augment reactant adsorption at higher catalyst concentrations, thus limiting further enhancement in cyclohexanone oxime conversion. Consequently, all subsequent experiments were conducted utilizing 0.15 g of catalyst.

Cyclohexanone oxime's molecular size, which is roughly 6 Å, is very comparable to the zeolitic ZSM-5 structure's micropore diameter (Linares et al., 2017). This implies that the reaction most likely happens at the mesopore/external surface or close to the micropore entrances (Chu et al., 2017). The augmentation in catalyst quantity doesn't notably influence the product selectivity in the Beckmann rearrangement of cyclohexanone oxime. The superior selectivity of ε-caprolactam over other products arises from the opening of external pores, expediting the rapid desorption of products (Marthala et al., 2006). This, in turn, hinders subsequent reactions, such as the generation of byproducts like hydrolysis and polymerization products, which could compromise ε-caprolactam selectivity and induce catalyst deactivation.

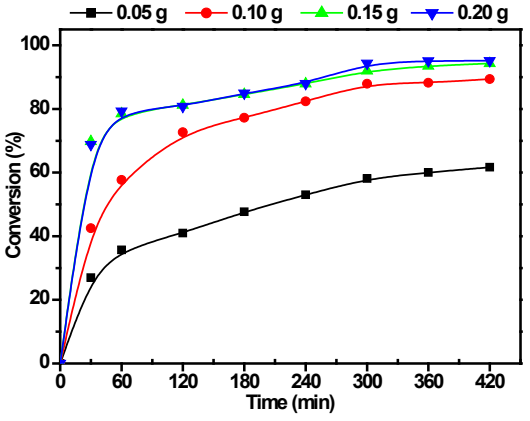


**Figure 8.** Effect of catalyst quantity on % conversion in Beckmann rearrangement of cyclohexanone oxime using ZSM-5 (50)-NP.24/c catalyst.
(Reaction conditions: catalyst- ZSM-5 (50)-NP.24/c; Concentration of cyclohexanone oxime (100 mmol); temperature-120°C; run time, 5 h; atmospheric pressure).

### 3.6.4. Effect of Reaction Temperature

With 0.10 g of ZSM-5 (50)-NP.24/c catalyst, the Beckmann rearrangement of cyclohexanone oxime to caprolactam was studied in the 110–140°C temperature range and the results are illustrated in **Fig. 9**. A notable enhancement in oxime conversion is observed as the reaction temperature rises, increasing from 45.8% at 110°C to 87.9% at 120°C. However, beyond 120°C, no appreciable improvement in conversion is

seen. The selectivity towards e-caprolactam remains consistently high, hovering around 95%, and shows no substantial variation with temperature. This stability in selectivity is attributed to the absence of dehydrogenation and fragmentation across the studied temperature range. Similar behaviors have been documented in previous studies on liquid-phase reactions catalyzed by zeolites (Wang et al., 2023).

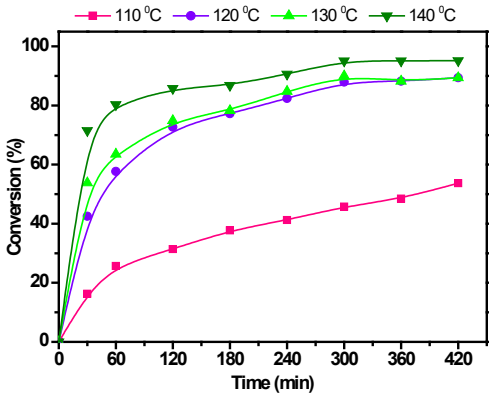


**Figure 9.** Effect of reaction temperature on % conversion in Beckmann rearrangement of cyclohexanone oxime using ZSM-5 (50)-NP.24/c catalyst. (Reaction conditions: catalyst-0.10 g of ZSM-5 (50)-NP.24/c; Concentration of cyclohexanone oxime (100 mmol); run time, 5 h; atmospheric pressure)

### *3.6.5. Reusability of Catalyst*

The reusability of ZSM-5 nanoparticles, aged at 80°C for 24 h (denoted as ZSM-5 (50)-NP.24/c), was investigated through three cycles under similar reaction conditions, incorporating the application of fresh catalyst and the data is presented in **Table** 1. Post-use, the catalyst underwent centrifugation, benzonitrile washing, and subsequent drying at 120°C for 6 h, preparatory to its reuse in subsequent batches. The data shows no significant change in oxime conversion and selectivity over three cycles. Thus, it can be inferred that the catalyst remains stable and suitable for reuse. Prior research has demonstrated that the production of byproducts, such as those resulting from hydrolysis and polymerization, can have a substantial effect on caprolactam's selectivity and aid in the deactivation of the catalyst (Kumar and Chowdhury, 2014). In this study, a distinctive synthesis procedure was employed, resulting in a catalyst with enhanced properties for the Beckmann rearrangement of cyclohexanone oxime. Remarkably, the catalyst exhibited no signs of deactivation over three consecutive runs.

**Table 1.** Reusability of ZSM-5(50)-24/con conversion (%) and selectivity (%) in Beckmann rearrangement of cyclohexanone oxime.

| Conversion (%) | | | Selectivity (%) | |
|---|---|---|---|---|
| **Fresh** | **First Reuse** | **Second Reuse** | **ε Caprolactam** | **Cyclohexanone** |
| 87.9 | 87.3 | 87.1 | 95 | 5 |

(Reaction conditions: catalyst- 0.10 g of ZSM-5(50)-24/c; Concentration of cyclohexanone oxime (100 mmol); temperature-120 oC; run time, 5 h; atmospheric pressure)

## 4. CONCLUSIONS

ZSM-5 nanoparticles can be effectively used as a catalyst in a moderate catalytic liquid-phase Beckmann rearrangement of cyclohexanone oxime to ε-caprolactam which is environmentally safe and produces great conversion and selectivity. Various reaction parameters, including the concentration of cyclohexanone oxime, catalyst quantity, reaction temperature, and catalyst reusability, were meticulously optimized. Notably, the concentrated nanoparticle ZSM-5 catalyst aged at 80°C (ZSM-5(50)-24/c) exhibited remarkable activity and selectivity for ε-caprolactam production, with negligible formation of byproducts resulting from dehydrogenation and fragmentation under standard reaction conditions. The following were found to be the ideal circumstances for the Beckmann rearrangement of cyclohexanone oxime: 0.10 g of ZSM-5(50)-24/c catalyst, cyclohexanone oxime concentration of 100 mmol, reaction temperature of 120°C, a reaction time of 5 h, and atmospheric pressure. This catalytic system is not only environmentally benign but also facile to separate, and the catalyst can be efficiently reused. Such a method holds significant promise for chemical industries, offering a cleaner synthesis route for ε-caprolactam production, thereby contributing to sustainable practices.

 https://doi.org/10.37819/nanofab.10.2079

## Funding

This research received no external funding.

## Data Availability

The data used to support the findings of this study are included in the article.

## Conflicts of Interest

The authors declare that they have no conflicts of interest.

## Authors' Contribution

Conceptualization, L.S. Roselin and R. Selvin.; Methodology R. Selvin, and R. Savidha; Validation, Walaa A., and Khadijah H.A.; Formal Analysis, L.S. Roselin and R.C. Hsiao; Investigation, R. Savidha and Walaa A.; Resources, R.C. Hsiao; Data Curation, Khadijah H.A. and R.C. Hsiao; Writing – Original Draft Preparation, L.S. Roselin, and R. Savidha; Writing – Review & Editing, Khadijah H.A. Walaa A. and R. Selvin; Visualization, S.G. Ramaraj; Supervision, R. Selvin; Project Administration, L.S. Roselin.

## Reference

Aerts, A., Isacker, A. V., Huybrechts, W., Kremer, S. P. B., Kirschhock, C. E. A., Collignon, F., Houthoofd, K., Denayer, J. F. M., Baron, G. V., Marin, G. B., Jacobs, P.A., Martens, J. A., (2004). Decane hydroconversion on bifunctional Zeogrid and nano-zeolite assembled from aluminosilicate nanoslabs of MFI framework type. *Appl. Catal. A: Gen. 257*(1), 7–17. https://doi.org/10.1016/S0926-860X(03)00592-1

Ando, T., Brown, S. J., Clark, J. H., Cork, D. G., Hanafusa, T., Ichihara, J., Miller, J. M., Robertson, M. S., (1986). Alumina-supported fluoride reagents for organic synthesis: optimisation of reagent preparation and elucidation of the active species. *Journal of the Chemical Society, Perkin Transactions 2*, (8), 1133–1139. https://doi.org/10.1039/P29860001133

Anilkumar, M., Hoelderich, W. F., (2012). New non-zeolitic Nb-based catalysts for the gas-phase Beckmann rearrangement of cyclohexanone oxime to caprolactam. *J. Catal.* 293, 76–84. https://doi.org/10.1016/j.jcat.2012.06.007

Aucejo, A., Burguet, M. C., Corma, A., Fornes, V., (1986). Beckman rearrangement of cyclohexanone-oxime on HNaY zeolites: kinetic and spectroscopic studies. *Applied Catalysis, 22*(2), 187–200. https://doi.org/10.1016/S0166-9834(00)82628-7

Beaumont, R., Barthomeuf, D., (1972). X, Y, aluminum-deficient and ultrastable faujasite-type zeolites II. Acid strength and aluminum site reactivity. *J. Catal. 27*(1), 45–51. https://doi.org/10.1016/0021-9517(72)90151-0

Centi, G., Perathoner, S., (2011). Creating and mastering nano-objects to design advanced catalytic materials. *Coordination Chemistry Reviews. 255*(13-14), 1480–1498. https://doi.org/10.1016/j.ccr.2011.01.021

Chandrasekhar, S., Gopalaiah, K. (2003). Ketones to amides via a formal Beckmann rearrangement in "one pot": a solvent-free reaction promoted by anhydrous oxalic acid. Possible analogy with the Schmidt reaction. *Tetrahedron Lett. 44*(40), 7437–7439. https://doi.org/10.1016/j.tetlet.2003.08.038

Chandrasekhar, S., Gopalaiah, K., (2002). Beckmann rearrangement of ketoximes on solid metaboric acid: a simple and effective procedure. *Tetrahedron Lett. 43*(13), 2455–2457. https://doi.org/10.1016/S0040-4039(02)00282-4

Chang, A., Yang, T. C., Chen, M. Y., Hsiao, H. M., & Yang, C. M. (2020). Hierarchical zeolites comprising orthogonally stacked bundles of zeolite nanosheets for catalytic and adsorption applications. *Journal of Hazardous Materials*, 400, 123241. 10.1016/j.jhazmat.2020.123241

Choi, M., Cho, H.x S., Srivastava, R., Venkatesan, C., Choi, D. H., Ryoo, R. (2006). Amphiphilic organosilane-directed synthesis of crystalline zeolite with tunable mesoporosity. *Nature Mater 5*, 718–723. https://doi.org/10.1038/nmat1705

Chu, Y., Li, G., Huang, L., Yi, X., Xia, H., Zheng, A., Deng, F., (2017). External or internal surface of H-ZSM-5 zeolite, which is more effective for the Beckmann rearrangement reaction? *Catal. Sci. Technol. 7*(12), 2512–2523. https://doi.org/10.1039/C7CY00377C

Conesa, T.D., Mokaya, R., Yang, Z., Luque, R., Campelo, J.M., Romero, A.A., (2007). Novel mesoporous silicoaluminophosphates as highly

active and selective materials in the Beckmann rearrangement of cyclohexanone and cyclododecanone oximes. *J. Catal. 252*(1), 1–10. https://doi.org/10.1016/j.jcat.2007.09.006

Corma, A. (2003). State of the art and future challenges of zeolites as catalysts. *Journal of Catalysis, 216*(1-2), 298–312. https://doi.org/10.1016/S0021-9517(02)00132-X

Corma, A., Garcia, H., Primo, J., Sastre, E., (1991). Beckmann rearrangement of cyclohexanone oxime on zeolites. *Zeolites, 11*(6), 593–597. https://doi.org/10.1016/S0144-2449(05)80010-7

Curtin, T., McMonagle, J. B., Hodnett, B. K., (1992). Influence of boria loading on the acidity of B2O3/Al2O3 catalysts for the conversion of cyclohexanone oxime to caprolactam. Appl. *Catal. A: Gen., 93*(1), 91–101. https://doi.org/10.1016/0926-860X(92)80296-O

Curtin, T., Mcmonagle, J. B., Ruwet, M., Hodnett, B. K., (1993). Deactivation and Regeneration of Alumina Catalysts for the Rearrangement of Cyclohexanone Oxime into Caprolactam. *J. Catal., 142*(1), 172–181. https://doi.org/10.1006/jcat.1993.1199

Dai, L.-X., Hayasaka, R., Iwaki, Y., Koyano, K. A., & Tatsumi, T., (1996). Vapour phase Beckmann rearrangement of cyclohexanone oxime catalysed by Hβ zeolite. *Chem. Commun. 9*, 1071–1072. https://doi.org/10.1039/CC9960001071

Dai, L.-X., Koyama, K., Miyamoto, M., Tatsumi, T., (1999). Highly selective vapor phase Beckmann rearrangement over H-USY zeolites. *Appl. Catal. A: Gen. 189*(2), 237–242. https://doi.org/10.1016/S0926-860X(99)00280-X

Davis, Jr., J. H., Fox, P. A., (2003). From curiosities to commodities: ionic liquids begin the transition. *Chem. Commun.* (11), 1209–1212. https://doi.org/10.1039/B212788A

De Moor, P.-P. E. A., Beelen, T. P. M., van Santen, R. A., (1999). In situ Observation of Nucleation and Crystal Growth in Zeolite Synthesis. A Small-Angle X-ray Scattering Investigation on Si-TPA-MFI. *The Journal of Physical Chemistry B, 103*(10), 1639–1650. https://doi.org/10.1021/jp982553q

Deng, Y.-Q., Yin, S.-F., Au, C.-T., (2012). Preparation of Nanosized Silicalite-1 and Its Application in Vapor-Phase Beckmann Rearrangement of Cyclohexanone Oxime. *Ind. Eng. Chem. Res. 51*(28), 9492–9499. https://doi.org/10.1021/ie3001277

Dupont, J., de Souza, R. F., Suarez, P. A. Z., (2002). Ionic Liquid (Molten Salt) Phase Organometallic Catalysis. *Chem. Rev. 102*(10), 3667–3692. https://doi.org/10.1021/cr010338r

Dusselier, M., Van Wouwe, P., Dewaele, A., Jacobs, P. A., Sels, B. F. (2015). Shape-selective zeolite catalysis for bioplastics production. *Science, 349*(6243), 78–80. DOI: 10.1126/science.aaa7169

Elings, J. A., Ait-Meddour, R., Clark, J. H., Macquarrie, D. J. (1998). Preparation of a silica-supported peroxycarboxylic acid and its use in the epoxidation of alkenes†. *Chemical Communications*, (24), 2707–2708. https://doi.org/10.1039/A807517D

Flowers, G. C., Lindley, S., Leffler, J. E., (1984). Variability of silica surfaces as reaction media. *Tetrahedron Letters, 25*(44), 4997–4998. https://doi.org/10.1016/S0040-4039(01)91100-1

Ge, C., Sun, X., Lian, D., Li, Z., & Wu, J., (2021). Controllable Synthesis and Structure-Performance Relationship of Silicalite-1 Nanosheets in Vapor Phase Beckmann Rearrangement of Cyclohexanone Oxime. *Catal. Lett. 151*, 1488–1498 https://doi.org/10.1007/s10562-020-03404-8

González-Camuñas, N., Cantín, Á., Dawson, D. M., Lozinska, M. M., Martínez-Triguero, J., Mattock, J., Cox, P. A., Ashbrook, S. E., Wright, P. A. and Rey, F. (2024). Synthesis of the large pore aluminophosphate STA-1 and its application as a catalyst for the Beckmann rearrangement of cyclohexanone oxime. *Journal of Materials Chemistry A, 12*(25), pp. 15398–15411. https://doi.org/10.1039/D4TA01132E

Hölderich, W. F., Röseler, J., Heitmann, G., Liebens, A. T. (1997). The use of zeolites in the synthesis of fine and intermediate chemicals. *Catalysis Today, 37*(4), 353–366. https://doi.org/10.1016/S0920-5861(97)81094-2

Ichihashi, H., Ishida, M., Shiga, A., Kitamura, M., Suzuki, T., Suenobu, K., Sugita, K., (2003). The Catalysis of Vapor-Phase Beckmann Rearrangement for the Production of ε-Caprolactam. *Catalysis Surveys from Asia, 7*(4), 261–270. https://doi.org/10.1023/B:CATS.0000008165.80991.05

Ishida, M., Suzuki, T., Ichihashi, H., Shiga, A., (2003). Theoretical study on vapour phase Beckmann rearrangement of cyclohexanone oxime over a high silica MFI zeolite. *Catalysis Today, 87*(1-4), 187–194. https://doi.org/10.1016/j.cattod.2003.10.021

Jacobs, P. A., Derouane, E. G., Weitkamp, J. (1981). Evidence for X-ray-amorphous zeolites. *Journal of the Chemical Society, Chemical Communications*, (12), 591–593. https://doi.org/10.1039/C39810000591

Jacobs, P.A. (1977). Carboniogeiic Activity of Zeolites, Elsevier, Amsterdam.

Jang, J., Lee, H. S., Kim, J. W., Kim, S. Y., Kim, S. H., Hwang, I., Kang, B. J., Kang, M. K. (2019). Facile and cost-effective strategy for fabrication of polyamide 6 wrapped multi-walled carbon nanotube via anionic melt polymerization of ε-caprolactam. *Chem. Eng. J.*, 373, 251–258. https://doi.org/10.1016/j.cej.2019.05.044

Katada, N., Tsubouchi, T., Niwa, M., Murakami, Y., (1995). Vapor-phase Beckmann rearrangement over silica monolayers prepared by chemical vapor deposition. *Appl. Catal. A: Gen. 124*(1), 1–7. https://doi.org/10.1016/0926-860X(94)00257-6

Kent J. E. Riegel's Handbook of industrial Chemistry, 8th Ed., Van Nostrand, New York, (1983), p. 402

Khayyat, S. A., Selvin, R., Umar, A., (2017). Beckmann Rearrangement of Cyclohexanone Oxime Using Nanocrystalline Titanium Silicalite-1 (TS-1). *J. Nanosci. Nanotechnol., 17*(3), 2170–2176. https://doi.org/10.1166/jnn.2017.12724

Kiely-Collins, H. J., Sechi, I., Brennan, P. E., McLaughlin, M. G. (2018). Mild, calcium catalysed Beckmann rearrangements. *Chem. Commun. 54*(6), 654–657. https://doi.org/10.1039/C7CC09491D

Kirk-Othmer, Encyclopedia of Chemical Technology, vol. 19, fourth ed., Wiley, New York, 1992, 493.

Kragten, D. D., Fedeyko, J. M., Sawant, K. R., Rimer, J. D., Vlachos, D. G., Lobo, R. F., Tsapatsis, M., (2003). Structure of the Silica Phase Extracted from Silica/(TPA)OH Solutions Containing Nanoparticles. *The Journal of Physical Chemistry B, 107*(37), 10006–10016. https://doi.org/10.1021/jp035110h

Kremer, S. P. B., Kirschhock, C. E. A., Tielen, M., Collignon, F., Grobet, P. J., Jacobs, P. A., Martens, J. A., (2002). Silicalite-1 Zeogrid: A New Silica Molecular Sieve with Super- and Ultra-Micropores. *Advanced Functional Materials, 12*(4), 286. https://doi.org/10.1002/1616-3028(20020418)12:4<286::AID-ADFM286>3.0.CO;2-M

Kumar, R., Chowdhury, B. (2014). Comprehensive Study for Vapor Phase Beckmann Rearrangement Reaction over Zeolite Systems. *Industrial & Engineering Chemistry Research, 53*(43), 16587–16599. https://doi.org/10.1021/ie503170n

Leithall, R. M., Shetti, V. N., Maurelli, S., Chiesa, M., Gianotti, E., Raja, R. (2013). Toward understanding the catalytic synergy in the design of bimetallic molecular sieves for selective aerobic oxidations. *J. Am. Chem. Soc.* 2013, 135, 2915–2918. https://doi.org/10.1021/ja3119064

Lezcano-González, I., Boronat, M., & Blasco, T. (2009). Investigation on the Beckmann rearrangement reaction catalyzed by porous solids: MAS NMR and theoretical calculations. *Solid State Nucl. Magn. Reson. 35*(2), 120–129. https://doi.org/10.1016/j.ssnmr.2009.02.001

Li, W. C., Lu, A. H., Palkovits, R., Schmidt, W., Spliethoff, B., and Schüth, F. (2005). Hierarchically structured monolithic silicalite-1 consisting of crystallized nanoparticles and its performance in the Beckmann rearrangement of cyclohexanone oxime. 127(36), 12595–600. https://doi.10.1021/ja052693v

Linares, M., Vargas, C., García, A., Ochoa-Hernández, C., Čejka, J., García-Muñoz, R. A., Serrano, D. P., (2017). Effect of hierarchical porosity in Beta zeolites on the Beckmann rearrangement of oximes. *Catalysis Science & Technology*, 7(1), 181–190. https://doi.org/10.1039/C6CY01895E

Mao, D., Lu, G., Chen, Q., Xie, Z., Zhang, Y. (2001). Catalytic Performance of $B_2O_3/TiO_2$–$ZrO_2$ for Vapor-Phase Beckmann Rearrangement of Cyclohexanone Oxime: The Effect of Boria Loading. *Catalysis Lett.* 77, 119–124. https://doi.org/10.1023/A:1012787028360

Maronna, M. M., Kruissink, E. C., Tinge, J. T., Agar, D. W., & Hoelderich, W. F. (2016). Kinetic Study on Gas-Phase Beckmann Rearrangement of Cyclohexanone Oxime to ε-Caprolactam over a Silica-Supported Niobia Catalyst. *Ind. Eng. Chem. Res. 55*(5), 1202–1214. https://doi.org/10.1021/acs.iecr.5b04240

Marthala, V. R. R., Frey, J., Hunger, M., (2010). Accessibility and Interaction of Surface OH Groups in Microporous and Mesoporous Catalysts Applied for Vapor-Phase Beckmann Rearrangement of Oximes. *Catalysis Lett. 135*(1-2), 91–97. https://doi.org/10.1007/s10562-010-0274-7

Marthala, V.R.R., Jiang, Y., Huang, J., Wang, W., Gläser, R., Hunger, M. (2006). Beckmann

Rearrangement of 15N-Cyclohexanone Oxime on Zeolites Silicalite-1, H-ZSM-5, and H-[B] ZSM-5 Studied by Solid-State NMR Spectroscopy. *Am. Chem. Soc.*, *128*(46), 14812–14813. https://doi.org/10.1021/ja066392c

Marthala, V.R.R., Rabl, S., Huang, J., Rezai, SAS., Thomas, B., Hunger, M., (2008). In situ solid-state NMR investigations of the vapor-phase Beckmann rearrangement of 15N-cyclohexanone oxime on MFI-type zeolites and mesoporous SBA-15 materials in the absence and presence of the additive 13C-methanol. *J. Catal. 257*(1), 134–141. https://doi.org/10.1016/j.jcat.2008.04.014

Marzianom, N.C., Ronchin L., Tortato, C. Vavasori A., Badetti C., (2007). Catalyzed Beckmann rearrangement of cyclohexanoneoxime in heterogeneous liquid/solid system Part 1: Batch and continuous operation with supported acid catalysts. *Journal of Molecular Catalysis A: Chemical* 277, 221–232. https://doi.org/10.1016/j.molcata.2007.07.046

Narasaka, K., Kusama, H., Yamashita, Y., Sato, H., (1993). Beckmann Rearrangement Catalyzed by the Combined Use of Tetrabutylammonium Perrhenate (VII) and Trifluoromethanesulfonic Acid. *Chemistry Lett. 22*(3), 489–492. https://doi.org/10.1246/cl.1993.489

Nimisha, N. P., Narendranath S. B., Sakthivel A., (2024). In situ preparation of a nickel-oxy-hydrxide decorated ITQ-2 composite: a hydrodeoxygenation catalyst. *Chem. Commun.*, (60), 1480-1483. https://doi.org/10.1039/D3CC05427F

Palkovits, R., Schmidt, W., Ilhan, Y., Erdem-Şenatalar, A., Schüth, F. (2009). Crosslinked TS-1 as stable catalyst for the Beckmann rearrangement of cyclohexanone oxime. *Microporous and Mesoporous Materials*, *117*(1-2), 228–232. https://doi.org/10.1016/j.micromeso.2008.06.041

Park, H., Bang, J., Park, H., Kim, J., Kim, J. C., Park, J. Y. and Ryoo, R. (2023). Surface silanol sites in mesoporous MFI zeolites for catalytic Beckmann rearrangement. *Catalysis Science & Technology*, *13*(11), pp. 3436–3444. https://doi.org/10.1039/D3CY00543G

Polshettiwar, V., Varma, R. S., (2010). Green chemistry by nano-catalysis. *Green Chemistry, 12*(5), 743–754. https://doi.org/10.1039/B921171C

Poole, C. F., (2004). Chromatographic and spectroscopic methods for the determination of solvent properties of room temperature ionic liquids. *Journal of Chromatography A*, *1037*(1-2), 49–82. https://doi.org/10.1016/j.chroma.2003.10.127

Potter, M. E., O'Malley, A. J., Chapman, S., Kezina, J., Newland, S. H., Silverwood, I. P., Mukhopadhyay, S., Carravetta, M.,Mezza, T.M., Parker, S.F., Catlow C.R.A., Raja, R., (2017). Understanding the Role of Molecular Diffusion and Catalytic Selectivity in Liquid-Phase Beckmann Rearrangement. *ACS Catalysis, 7*(4), 2926–2934. https://doi.org/10.1021/acscatal.6b03641

Potter, M. E., Cholerton, M. E., Kezina, J., Bounds, R., Carravetta, M., Manzoli, M., Gianotti, E., Lefenfeld, M., Raja, R. (2014). Role of Isolated Acid Sites and Influence of Pore Diameter in the Low-Temperature Dehydration of Ethanol. *ACS Catalysis*, *4*(11), 4161–4169. https://doi.org/10.1021/cs501092b

Raja, R., Potter, M. E., Newland, S. H., (2014). Predictive design of engineered multifunctional solid catalysts. *Chem. Commun.*, 50(45), 5940–5957. https://doi.org/10.1039/C4CC00834K

Ravishankar, R., Kirschhock, C. E. A., Knops-Gerrits, P.-P., Feijen, E. J. P., Grobet, P. J., Vanoppen, P., De Schryver, F.C., Miehe, G., Fuess, H., Schoeman, B.J., Jacobs, P.A., Martens, J. A. (1999). Characterization of Nanosized Material Extracted from Clear Suspensions for MFI Zeolite Synthesis. *The Journal of Physical Chemistry B*, *103*(24), 4960–4964. https://doi.org/10.1021/jp990296z

Regev, O., Cohen, Y., Kehat, E., Talmon, Y., (1994). Precursors of the zeolite ZSM-5 imaged by Cryo-TEM and analyzed by SAXS. *Zeolites*, *14*(5), 314–319. https://doi.org/10.1016/0144-2449(94)90103-1

Ren, R.X., Zueva, L., Ou, W., (2001). Formation of caprolactum via catalytic Beckmann rearrangment using $P_2O_5$ in ionic liquids. *Tetrahedron Lett.* 42, 8441–8443. https://doi.org/10.1016/S0040-4039(01)01850-0

Röseler, J., Heitmann, G., Hölderich, W. F. (1996). Vapour-phase Beckmann rearrangement using B-MFI zeolites. *Appl. Catal. A: Gen. 144*(1-2), 319–333. https://doi.org/10.1016/0926-860X(96)00127-5

Sahu, P., and Sakthivel, A. (2021). Zeolite-β based molecular sieves: A potential catalyst for esterification of biomass derived model compound levulinic acid. *Materials Science for Energy Technologies*, 4, 307–316. doi:10.1016/j.mset.2021.08.007

Sato, S., Urabe, K., and Izumi, Y., (1986). Vapor-phase Beckmann rearrangement over silica-supported boria catalyst prepared by vapor decomposition method. *J. Catal. 102*(1), 99–108. https://doi.org/10.1016/0021-9517(86)90144-2

Selvin, R., Hsu, H.-L., T.-M. Her., (2008). Acylation of anisole with acetic anhydride using ZSM-5 catalysts: Effect of ZSM-5 particle size in the nanoscale range. *Catal. Commun. 10*(2), 169–172. https://doi.org/10.1016/j.catcom.2008.08.013

Selvin, R., Rajarajeswari, G., Selva Roselin, L., Sadasivam, V., Sivasankar, B., Rengaraj, K., (2001). Catalytic decomposition of cumene hydroperoxide into phenol and acetone. *Appl. Catal. A: Gen. 219*(1-2), 125–129. https://doi.org/10.1016/S0926-860X(01)00674-3

Selvin, R., Sivasankar, B., Rengaraj, K., (1999). Kinetic studies on Friedel-Crafts acylation of anisole by clayzic. React. Kinet. *Catal. Lett. 67*(2), 319–324. https://doi.org/10.1007/BF02475778

Shabana, K. K., Narendranath, S. B., Nimisha, N. P., Venkatesha, N. J., Sheetal G., A. Sakthivel A. (2024). Temperature-programmed reduction method for stabilization of the inorganic framework of SAPO-37 materials: promising catalysts for MTBE production. *Chem. Commun.*, 60, 8688-8691. https://doi.org/10.1039/D4CC01839G

Sirijaraensre, J., Limtrakul, J., (2009). Effect of the acidic strength on the vapor phase Beckmann rearrangement of cyclohexanone oxime over the MFI zeolite: an embedded ONIOM study. *Phys. Chem. Chem. Phys. 11*(3), 578–585. https://doi.org/10.1039/B808662A

Smith, J. V. (1988). Topochemistry of zeolites and related materials. 1. Topology and geometry. *Chemical Reviews*, *88*(1), 149–182. https://doi.org/10.1021/cr00083a008

Takahashi, T., Kai, T. and Nakao, E., (2004). Catalyst deactivation in the Beckmann rearrangement of cyclohexanone oxime over HSZM-5 zeolite and silica-alumina catalysts. *Applied Catalysis A: General*, *262*(2), pp.137-142. https://doi.org/10.1016/j.apcata.2003.11.040

Thangaraj, A., Sivasanker, S. Ratnasamy P., (1992). Catalytic properties of titanium silicalites IV. Vapour phase beckmann rearrangement of cyclohexanone oxime. *J. Catal. 137*(1), 252–256. https://doi.org/10.1016/0021-9517(92)90154-A

Thorat, T. S., Yadav, V. M., Yadav, G. D., (1992). Esterification of phthalic anhydride with 2-ethylhexanol by solid superacidic catalysts. *Appl. Catal. A: Gen. 90*(2), 73–96. https://doi.org/10.1016/0926-860X(92)85050-L

Ushikubo, T., Wada, K., (1994). Vapor-Phase Beckmann Rearrangement over Silica-Supported Tantalum Oxide Catalysts. *J. Catal. 148*(1), 138–148. https://doi.org/10.1006/jcat.1994.1195

Van Grieken, R., Sotelo, J. L., Menéndez, J. M., Melero, J. A. (2000). Anomalous crystallization mechanism in the synthesis of nanocrystalline ZSM-5. *Microporous and Mesoporous Materials*, *39*(1-2), 135–147. https://doi.org/10.1016/S1387-1811(00)00190-6

Wang, B., Gu, Y., Luo, C., Yang, T., Yang, L., Suo, J. (2004). Sulfamic acid as a cost-effective and recyclable catalyst for liquid Beckmann rearrangement, a green process to produce amides from ketoximes without waste. *Tetrahedron Lett. 45*(17), 3369–3372. https://doi.org/10.1016/j.tetlet.2004.03.017

Wang, K., Wang, F., Zhai, Y., Wang, J., Zhang, X., Li, M., Jiang, L., Fan, X., Bing, C., Zhang, J., Zhang, X., (2023). Application of zeolite in Beckmann rearrangement of cyclohexanone oxime. *Molecular Catalysis.* 112881–112901. https://doi.org/10.1016/j.mcat.2022.112881

Wang, Z., Liu, B., Lin, J., (2013). Highly effective perovskite-type BaZrO3 supported Ru catalyst for ammonia synthesis. *Appl. Catal. A: Gen.*, 458, 130–136. https://doi.org/10.1016/j.apcata.2013.03.037

Wasserscheid, P., Keim, W. (2000). Ionic Liquids—New "Solutions" for Transition Metal Catalysis. *Angewandte Chemie*, *39*(21), 3772–3789. https://doi.org/10.1002/1521-3773(20001103)39:21<3772::AID-ANIE3772>3.0.CO;2-5

Welton, T., Wasserscheid, P. (2008). In Ionic Liquids in Synthesis; Wiley-VCH: Weinheim, 1. 265–268.

Xu, B.-Q., Cheng, S.-B., Jiang, S., Zhu, Q.-M., (1999). Gas phase beckmann rearrangement of cyclohexanone oxime over zirconia-supported boria catalyst. *Appl. Catal. A: Gen.*, *188*(1-2), 361–368. https://doi.org/10.1016/S0926-860X(99)00255-0

Yadav, G. D., Joshi, A. V., (2001). Etherification of tert-Amyl Alcohol with Methanol over Ion-Exchange Resin. *Org. Proc. Res. Dev.* 5, 408-414. https://doi.org/10.1021/op010018+

Yashima, T., Oka, N., Komatsu, T., (1997). Vapor phase Beckmann rearrangement of cyclohexanone

oxime on the zeolite catalysts. *Catalysis Today, 38*(2), 249–253. https://doi.org/10.1016/S0920-5861(97)00074-6

Yin, P., Nie, J., Wen, X., Li Z., Zhang D., Zhao X., Wang Y. (2024). Application of Mixed Acid-Modified Hollow TS-1 Zeolite to Vapor-Phase Beckman Rearrangement Reaction. *Catal Lett*, 154, 6035–6048. https://doi.org/10.1007/s10562-024-04780-1

Zhang, D., Wang, R., Yang, X., Yao, W., (2010). Vapor-phase Beckmann rearrangement of cyclohexanone oxime over phosphorus modified Si-MCM-41. *React. Kinet. Mech. Catal. 101*(2), 455–463. https://doi.org/10.1007/s11144-010-0226-7

Zhang, X.-F., Zhang, K., Zhang, X., Feng, Y., & Yao, J. (2018). Controlled synthesis of hierarchical beta zeolite through design template to enhance gas-phase beckmann rearrangement performance. *Microporous and Mesoporous Materials*, 272, 202–208. https://doi.org/10.1016/j.micromeso.2018.06.034